AUTOMATED 3D MESH GENERATION FOR EFFICIENT TORQUE COMPUTATION OF ELECTROSTATIC MICROMOTORS.

TB. Johansson, K. Hameyer, R. Belmans, *E. Freeman

Katholieke Universiteit. Leuven, E.E. Dept, Div. ESAT/ELEN,
Kard. Mercierlaan 94, B-3001 Heverlee, BELGIUM

*Imperial College of Science and Technology, E.E. Dept.
Exhibition Road, London SW7 3BT, UK

ABSTRACT

The ever increasing interest in micro mechanics stresses the demand for analysing tools which can provide design roles. By tool is understood a software tool, and this is for electrical machines, or electrical energy converters in general, normally a finite element package for electro magnetism. However, such a tool is very general and must be customised and/or combined with analytical or other numerical methods before it can provide information useful for a manufacturer of specific devices.
This paper discusses two new techniques for the analysis and the optimisation of electrostatic micromotors of the type variable capacitance motors. The first one is a 3D mesh generation technique specially developed for electrostatic micromotors, but general enough to be used for various other types of rotating motors. The second one is the generation and use of an equivalent circuit model to enhance and speed up the analysis based on finite element technique. The paper shows how these techniques have been automated and combined to accomplish optimisation of the average torque of variable capacitance micro motors.

INTRODUCTION.

Industry's interest in micro electro-mechanical systems is rapidly increasing. The very small scale, airgaps of 1 to 10 μm and overall dimensions less than 1 mm, makes the electrostatic field beneficial compared to the magnetic field. As a consequence, most of these micro devices are electrostatic energy converters. Due to new processes to manufacture microactuators and micromotors as e.g. "X-ray LIGA" Mohr et. al. (1), "Near UV Lithography" Engelman et. al. (2), "plasma etching" etc. the number of possible structures has grown as well as the precision with which they can be manufactured. As a consequence, there is an increasing need for better analysing tools. The demand is for them to be faster and more accurate but also more flexible and easy to use. This paper presents techniques which meet some of these requirements.

3D MOTOR MESHES

Building a 3D mesh is normally a time consuming process. However, numeric optimisation a large number of model evaluations is required. For micromotor structures, the required labour is even vaster since for every model the analysis normally must be carried out for a number of rotor positions, in order to obtain macroscopic parameters as torque and capacitance as functions of the rotor position. For most 3D finite element packages a new rotor position requires a new mesh to be generated. An automated mesh generation is therefore required. In this paper the fast extrusion-based 3D mesh generator is used. It is automated in such a way that a large number of different motor geometries can be generated, all having a fully arbitrary choice of the rotor position.

Periodic Geometries

All electrical rotating motors inherently possess some kind of periodicity. Typically each motor has a stator and a rotor where the geometric period, in degrees, is defined by the pole pitch τ_p. Each periodic geometry also has an extension within the pole pitch. This extension is referred to as the polar arc τ (fig. 1).

The pole pitch τ_p and the polar arc τ, makes it easy to

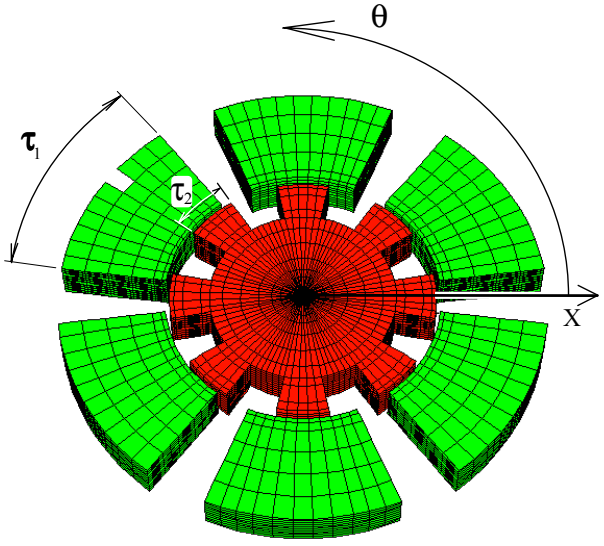

Fig. 1. 3D mesh of a 6/8 pole electrostatic radial flux micromotor.

describe where the sides of the stator teeth and rotor teeth, parallel with the rotor axis, are located in the motor. If the motor is scanned in the positive θ direction, see fig. 1, the following equations define the location of the front-sides and the back-sides of the stator teeth.

$$\left.\begin{aligned}\Theta^n_{1,front} &= \left(\frac{\tau_{p1}-\tau_1}{2}\right)+n\cdot\tau_{p1}\\ \Theta^n_{1,back} &= \left(\frac{\tau_{p1}+\tau_1}{2}\right)+n\cdot\tau_{p1}\end{aligned}\right\} \quad (1)$$

$$\text{where}\quad n=0,1,2,\ldots\frac{360°-\tau_{p1}}{\tau_{p1}}$$

The reference point for θ is chosen in the middle between two stator teeth. By introducing the offset angle α accounting for the rotor position, the same may be done for the rotor.

$$\left.\begin{aligned}\Theta^n_{2,front} &= \left(\frac{\tau_{p2}-\tau_2}{2}\right)+n\cdot\tau_{p2}+\alpha_2\\ \Theta^n_{2,back} &= \left(\frac{\tau_{p2}+\tau_2}{2}\right)+n\cdot\tau_{p2}+\alpha_2\end{aligned}\right\} \quad (2)$$

$$\text{where}\quad n=0,1,2,\ldots\frac{360°-\tau_{p2}}{\tau_{p2}}$$

Subscripts 1 and 2 indicate parameters for the stator and rotor respectively. In the general case, the motor geometry can be split into more than 2 periodic geometries.

Extrusion by rotation

The 3D meshes are built using an extrusion technique. With this technique 2D meshes, placed at different locations in space, are generated and connected resulting in the 3D mesh. A reference 2D mesh is referred to as the baseplane, see fig. 2. Each plane is applied with extrusion data describing its position in space. The extrusion technique, discussed here, uses only rotation around the y-axis, thus θ, to define the extrusion data. One vertical side of the base-plane coincides with the global y-axis. Since each copy of the base-plane gets the θ parameter as extrusion data, one of the vertical sides of all planes also coincide, with the global y-axis, i.e. the centre of the rotor shaft (fig. 3).

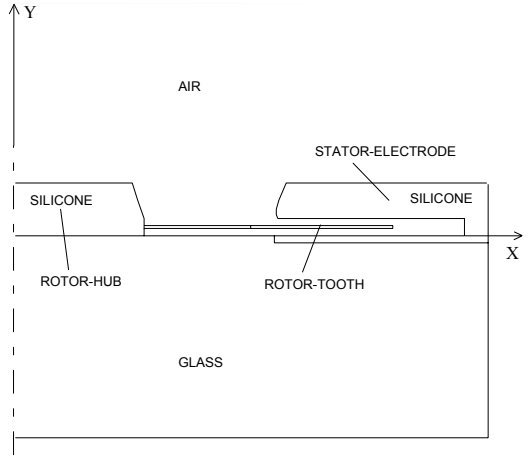

Fig. 2. Base-plane used when generating model of figure 3.

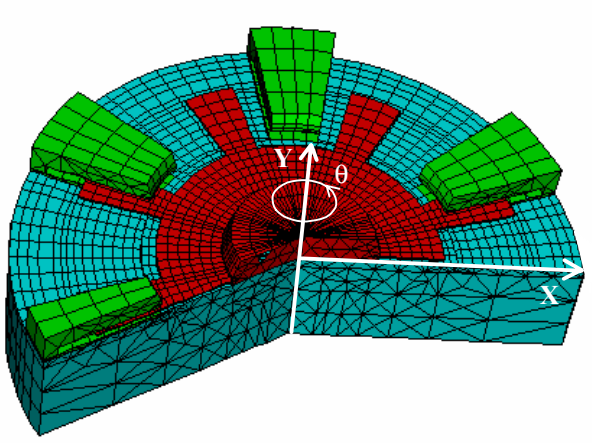

Fig. 3 Piece of a motor mesh built by altering the material properties, and/or the constraints, of the base-plane depending on the angle θ.

Using (1) and (2), knowing the number of poles, the polar arc τ of stator and rotor, and the rotor position α, it is easy to find where planes must be located. For each of the periodic geometries 4 different types of actions, sequence of relabeling and/or constraining, are defined. Relabeling defines material properties and constraining defines equipotential surfaces. Types 1 and 2 define a front and a backside respectively, of a tooth. Types 3 and 4 define a plane inside or outside of a tooth. Thus the maximum number of different plane-types required to construct a model is 4^N, where N is the number of periodic geometries in the model. These planes are generated in advance and are sufficient to define all possible combinations of

τ_p, τ and α.

Once the planes are generated the remaining task is to find at what angle which kind of plane must be located. This is performed with repetitive use of (1) and (2) and a sorting algorithm. This sorting algorithm finds what the next plane must be from knowing the previous one. A front-plane must be followed by and inside-plane, an inside-plane by a back-plane and so on. The angle between two consecutive planes has to be chosen depending on the size of the elements in the base-plane and the required aspect ratio of the 3D elements, the tetrahedrons. The aspect ratio is defined as the quote of the shortest and the longest side of a tetrahedron. This value may not exceed certain limits, not to negatively influence the accuracy of the solving process. This implies that the same kind of planes sometimes has to be repeated with the required angle between them in order to improve the aspect ratio of the tetrahedrons. This is automatically controlled.

Performance of model generator

The major advantage of automating the extrusion-based mesh generator, rather than a solid modeller, is speed. To generate a motor model with approximately 100'000 tetrahedrons takes, from the instant that the parameters are entered to the model is built ready for the solver, less than 10 minutes on a HP715. Once the different kinds of planes are generated, it takes always less then 5 min. This should be compared with typically more than 45 min for a solid modeller. The second reason is reliability. The extrusion technique does not make use of any iterative process that might for some geometries not converge. If the input data are valid the extrusion technique guaranties a valid mesh. This is very important for an optimisation process, that might need one or more days to find the final result. Intermediate results not valid due to unsuccessful mesh generation or a total termination of the optimisation process has to be avoided by all means.

OPTIMISATION

One of the most attractive possibilities that the automatic mesh generation described here offers, is optimisation. The geometry of the micromotors from fig. 1 and 3 is modelled by 4 design variables. The free parameters are the number of poles in stator and rotor, and the polar arcs of the stator electrodes and the rotor teeth. However, an optimisation is performed varying only the last two of these design variables and for each combination calculate the electric torque. Having a baseplane (fig. 2), the mesh generation technique is automated to generate a 3D motor mesh with the four design variables and the rotor position as the only input. This could be enough to automate the optimisation of a number of motors, having the same baseplane but different number of poles. Due to the choice to optimise with the average torque as the quality function, the automatic mesh generator is not quite enough. To optimise using the average torque does not only require one torque value for each rotor position but as many torque values as there are possible or interesting excitations. Only if the best excitation for each rotor position is used, the optimisation is meaningful. However, for each new excitation the finite element program must find a new solution, and would thus be a very time expensive optimisation. To overcome this problem an equivalent circuit technique is developed.

EQUIVALENT CIRCUIT MODEL

The information gained from two different excitations over the rotor positions is sufficient to create an equivalent circuit describing the motor geometry. The equivalent circuit used for a 6/8 pole motor is shown in fig. 4 and consists of 12 capacitors, two times the number of stator electrodes (poles). Their capacitance varies with the rotor position α. There are only two principally different capacitances. Writing $C_k^{SR}(\alpha)$ for

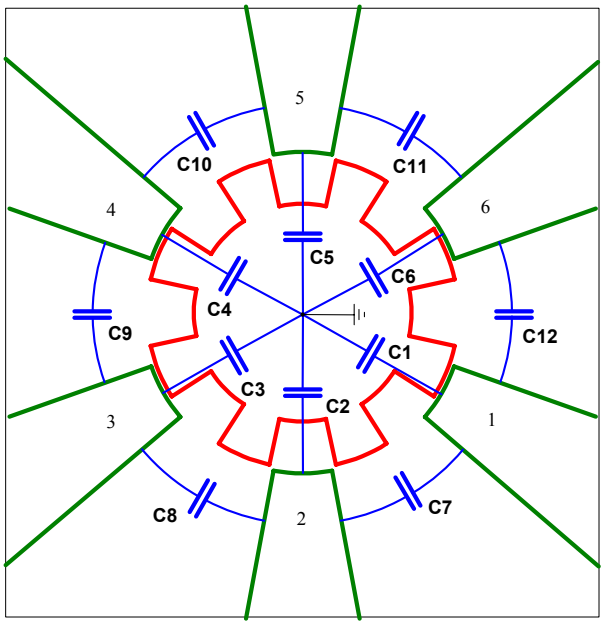

Fig. 4. Equivalent circuit for an electrostatic motor with 6 stator poles.

the capacitance between stator electrode k and the rotor, C1 to C6, and $C_k^{SS}(\alpha)$ for the capacitance between stator electrode k and the next stator electrode, C7 to C12, it can readily be seen that the difference between capacitances with different index k is only a phase shift equal to a multiple of the stator pole pitch τ_{p2}. Finding the energy stored in a capacitor from (3), and calculating the stored energy in the motor, for two different excitations and for n rotor positions, the system of equations (4) can be solved.

$$W_e = \frac{1}{2} C V^2 \tag{3}$$

$$\left.\begin{aligned} W_e(\alpha_1) &= \tfrac{1}{2}\sum_{k=1}^{n_{p1}}\left[C_k^{SR}(\alpha_1) V_k^2 + C_k^{SS}(\alpha_1)\cdot\left(V_{k+1}-V_k\right)^2 \right] \\ &\bullet \\ &\bullet \\ &\bullet \\ W_e(\alpha_n) &= \tfrac{1}{2}\sum_{k=1}^{n_{p1}}\left[C_k^{SR}(\alpha_n) V_k^2 + C_k^{SS}(\alpha_n)\cdot\left(V_{k+1}-V_k\right)^2 \right] \end{aligned}\right\} \tag{4}$$

where: $V_{k+1} = V_1$

$n_{p1} =$ number of stator electrodes

$n =$ number of rotor positions

Once $C_k^{SR}(\alpha)$ and $C_k^{SS}(\alpha)$ are found the torque is calculated using an analytic differentiation.

$$T_V(\alpha) = \frac{\partial W_e(\alpha)}{\partial \alpha} \tag{5}$$

The Best Excitation Sequence

Having the equivalent circuit any kind of excitation wave form can easily be applied. A block shaped wave form, simulating switching, is applied throughout the optimisation. To avoid or at least minimise radial forces on the rotor shaft, the motors have to be excited symmetrically. Figure 5 shows the possible symmetric excitations of a motor with 6 stator electrodes, where the dark electrodes are excited to V Volt and the white electrodes, and the rotor, are kept at reference potential.

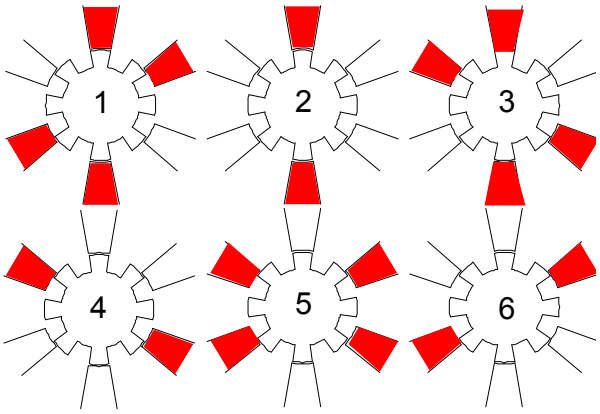

Fig. 5. Possible symmetric excitations of a motor with six electrodes.

By applying these excitations to the equivalent circuit, the torque characteristic as a function of the rotor position can be calculated. Fig. 6 shows the torque produced over one electric period for the six different excitations from fig. 5. By switching from one excitation to another, at the crossovers marked by arrows, the optimum excitation sequence is achieved. The average torque T_{av} is then calculated by integrating the curve always following the highest torque. The torque ripple T_{rpl} is given by

$$T_{rpl} = \frac{T_{max} - T_{min}}{T_{av}} \qquad (6)$$

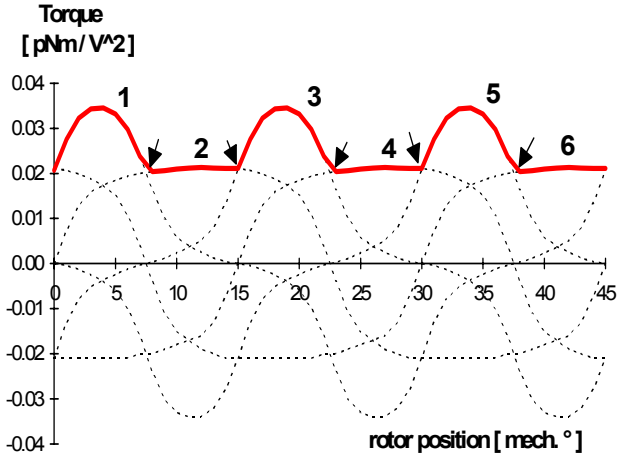

Fig. 6. Static torque over one electric period for 6 different excitations of a 6/8 pole motor.

RESULTS

Four different types of micromotors have been optimised. Two radial flux micromotors and two axial flux micromotors. For both types of motors two different pole configurations are considered, the 6/8 pole and the 6/4 pole configuration. For each of these designs the optimisation is performed with respect to the average electric torque and the design variables, the polar arc of both stator and rotor. Due to constraints resulting from the manufacturing conditions the other design variable are set to fixed values. For the motor from fig. 1 the air gap is fixed to 10 µm, the rotor height to 100 µm and the outer diameter of the rotor to 600 µm. For the motor from fig. 3 the air gap is fixed to 3 µm, the rotor thickness to 4 µm and the outer diameter of the rotor to 320 µm. Tables 1 and 2 show the results of the optimisations.

TABLE 1 - Radial flux motors with a rotor height of 100 µm, a rotor diameter of 600 µm and an airgap of 10 µm.

	6/8 pole configuration		**6/4 pole configuration**	
	motor with max. T_{av}	motor with min. T_{rpl}	motor with max. T_{av}	motor with min. T_{rpl}
T_{av} $\left[\frac{pNm}{V^2}\right]$	0.028	0.025	0.035	0.029
T_{rpl} [%]	63	28	81	26
τ_{p1} [°]	18.0	18.0	42.0	30
τ_{p2} [°]	21.6	13.5	40.5	38.7

Table 1 shows that the for the radial flux motors, the 6/4 pole configuration is superior to the 6/8 pole. The maximum average torque from the 6/4 pole motor is 25% higher then that from the strongest 6/8 pole motor, and the motor with the lowest torque ripple is also a 6/4 pole motor.

TABLE 2 - Axial flux motors with a rotor thickness of 4 µm, a rotor diameter of 320 µm and an airgap of 3 µm.

6/8 pole configuration		**6/4 pole configuration**	
motor with max. T_{av}	motor with min. T_{rpl}	motor with max. T_{av}	motor with min. T_{rpl}

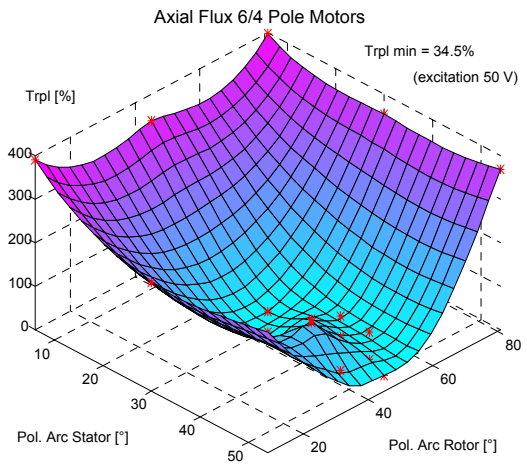

Fig. 8. Torque ripple as a function of combinations of polar arcs in the stator and the rotor, for 6/4 pole axial flux motors.

$\mathbf{T_{av}}$ $\left[\frac{\text{pNm}}{\text{V}^2}\right]$	0.041	0.038	0.060	0.044
$\mathbf{T_{rpl}}$ [%]	56	22	130	35
τ_{p1} [°]	22.8	27.6	44.4	54
τ_{p2} [°]	22.5	22.5	37.8	48.6

For the axial flux motor, table 2 , the situation is less clear. Here, the average torque is 15% higher for the strongest 6/4 pole motor, but the lowest torque ripple is for a 6/8 pole motor and is 13 % lower than for the corresponding 6/4 pole motor. It is thus from these lists difficult to draw any extended conclusions. The following two figures give here a more clear picture on how the average torque and the torque ripple depend on

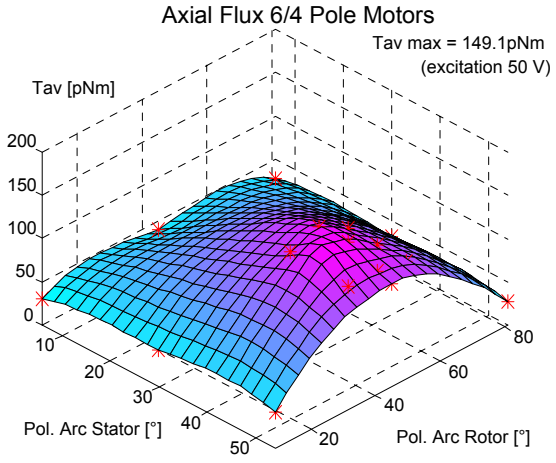

Fig. 7. Average torque as a function of combinations of polar arcs in the stator and the rotor, for 6/4 pole axial flux motors.

the design variables. In these pictures a surface fit has been applied to the evaluation points from the optimisation. Fig. 7 shows that the average torque has only one global maximum for the two design variables. However, the torque ripple does not have a clear global minima. Around a local maximum there are many combinations of the two design parameters that will give almost the same value.

CONCLUSIONS

This paper describes a technique to automate the generation of 3D meshes for electrostatic micromotors, and how this technique combined with an equivalent circuit technique provides the necessary tool to perform an optimisation of motors with respect to the average torque and/or torque ripple. Both the described model generation and equivalent circuit technique are well suited for further development.

ACKNOWLEDGEMENTS

The authors extend their gratitude to the Belgian Ministry of Scientific Research for granting the IUAP No. 51 on Magnetic Fields. Further our gratitude's to the council of the Belgian National Science Foundation, to the EC Commission for granting the Brite/Euram No. BE 3360, and to the Science Council of KU Leuven.

REFERENCES

1. J. Mohr, C. Burbaum, P. Bley, W. Menz and U. Wallrabe, 1990, MST '90 pp. 529-537.

2. G. Engelman, O. Ehrmann, R. Leutenbauer, H. Schmitz and H. Reichl, 1993 SPIE 2045, pp. 306-313.

3. W. Trimmer, R. Jebens, "Harmonic Electrostatic Motors", Sensors and Actuators, 20, 1989, pp. 17-224.

4. T.B. Johansson, M. Van Dessel R. Belmans W. Geysen, IEEE Trans. on Industry Applications Volume 30 Number 4, pp. 912 - 919.

5. D. A. Lowther P. P. Silvester 1985, "Computer Aided Design in Magnetics" Springer-Verlag, Berlin, New York, Heidelberg, Tokyo.